Available online at www.sciencedirect.com
ScienceDirect
Geomorphology 97 (2008) 35–51
GEOMORPHOLOGY
www.elsevier.com/locate/geomorph

Ice thickness and topographic relief in glaciated landscapes of the western USA

Simon H. Brocklehurst [a,*], Kelin X. Whipple [b], David Foster [a]

[a] School of Earth, Atmospheric and Environmental Sciences, The University of Manchester, Manchester M13 9PL, UK
[b] School of Earth and Space Exploration, Arizona State University, Tempe AZ 85287, USA

Received 18 September 2006; received in revised form 24 November 2006; accepted 23 February 2007
Available online 22 June 2007

Abstract

The development of relief in glaciated landscapes plays a crucial role in hypotheses relating climate change and tectonic processes. In particular, glaciers can only be responsible for peak uplift if they are capable of generating significant relief in formerly nonglaciated landscapes. Previous work has suggested that relief in glaciated landscapes should scale with the thickness of the ice. Here we summarise a field-based test of this hypothesis in two mountain ranges in the western United States, the Sierra Nevada, California, and the Sangre de Cristo Range, Colorado. These areas exhibit a range of degrees of glacial occupation during the Quaternary, including some drainage basins essentially unoccupied by ice, allowing a detailed exploration of how relief in different parts of a drainage basin evolves in response to glacial modification. We mapped last glacial maximum (LGM) trimlines to estimate the ice thickness at the equilibrium line altitude during the LGM, and determined several metrics of relief for drainage basins across the full spectrum of LGM ice extents. Comparison between measures of relief and ice thickness estimates indicates that relief production in glaciated mountain belts scales with ice thickness and consequently also drainage area. We extended our study to the Bitterroot Range in Idaho/Montana, and the Teton Range in Wyoming, for a more comprehensive understanding of sub-ridgeline relief, or 'missing mass'. This measure of mean relief is surprisingly little affected by either the degree of glacial modification or the total material removed by glaciers, but appears to be influenced by the more active tectonics of the Teton Range. While the effects of glacial modification on the landscape are clear (valley widening, hanging valley formation), the overall change in the relief structure of the mountain ranges studied here is surprisingly modest.

Keywords: Relief; Landscape evolution; Glacial geomorphology

1. Introduction

Surface processes are recognised as playing a crucial role in the development of mountain ranges (e.g., Molnar and England, 1990; Koons, 1995; Small and Anderson, 1998; Whipple et al., 1999; Willett, 1999). Rapid incision can potentially focus crustal strain (e.g., Koons, 1995; Zeitler et al., 2001) or alter near-surface geothermal gradients (e.g., Stüwe et al., 1994; Mancktelow and Grasemann, 1997), while changes in the relief structure of the landscape affect the isostatic response to erosion (e.g., Molnar and England, 1990; Montgomery, 1994; Small and Anderson, 1998; Whipple et al., 1999). The evolution of relief in response to climate change (and the onset of glaciation) is especially

* Corresponding author. Fax: +44 161 306 9361.
E-mail address: shb@manchester.ac.uk (S.H. Brocklehurst).

0169-555X/$ - see front matter © 2007 Elsevier B.V. All rights reserved.
doi:10.1016/j.geomorph.2007.02.037

crucial in the debate over potential linkages between apparently synchronous mountain uplift in the Himalayas, the western United States, and elsewhere, and late Cenozoic cooling (e.g., Molnar and England, 1990; Raymo and Ruddiman, 1992).

Molnar and England (1990) argued that the sedimentological and palynological evidence interpreted as indicating accelerated rates of late Cenozoic tectonism might instead reflect faster erosion caused by a cooler and/or stormier climate. They argued that this enhanced erosion resulted in the generation of relief, and subsequent isostatic uplift of various mountain ranges across the globe (Fig. 1). Whipple et al. (1999) argued that a stormier climate was unlikely to result in greater relief in the fluvial system, and furthermore made a theoretical argument that relief production by glaciers was likely to be more modest than that appealed to by Molnar and England (1990). Small and Anderson (1998) and Brocklehurst and Whipple (2002) presented evidence for only minor relief production by glaciers in the Wind River Range and the eastern Sierra Nevada (both in the western US), respectively. Montgomery (2002), however, found that glaciers in the Olympic Peninsula, Washington, have removed substantially more material than rivers, and that large alpine valleys have been deepened and widened following Pleistocene glaciation. Schuster et al. (2005) used $^{4}He/^{3}He$ thermochronometry to argue that the Klinaklini Valley in the southern Coast Mountains of British Columbia, Canada experienced significant relief production due to glacial erosion early in the Quaternary, but reduced valley erosion rates since then.

This paper reports the results of a field test of the hypothesis outlined by Whipple et al. (1999) that relief production by glaciers should scale with ice thickness (and thus in turn also reflects downvalley gradient). We recognise that the current state of the landscape reflects many glacial cycles with corresponding changes in glacier extents, dynamics and erosion rate distributions, but as an initial test of the hypothesis, we focus on the current snapshot of relief in glaciated landscapes, and how this relates to readily-mapped ice thickness and extent during the Last Glacial Maximum (LGM). We accept that this does not represent the "mean Quaternary" glaciers whose influence is most strongly reflected in the landscape (e.g., Porter, 1989; Brocklehurst and Whipple, 2002). Direct evidence is available from the Fennoscandian peninsula for mean extent (Kleman and Stroeven, 1997; Kleman et al., 2008-this volume) and ice thickness (Fredin, 2004), but in general these data are scarce. We mapped LGM trimlines and moraines in the Sierra Nevada, California, and the Sangre de Cristo Range, Colorado, and compared estimated centreline ice thicknesses at the LGM equilibrium line altitude (ELA) with measures of relief in these landscapes.

2. Background

"Relief" in any landscape varies with the scale over which it is measured. Accordingly, there are many different definitions for "relief" (Brocklehurst and Whipple (2002) gave a summary). For the purposes of evaluating the potential geodynamic response to erosion, the relevant measure is the "geophysical relief" (Small and Anderson, 1998). The geophysical relief is defined as the volume of material "missing" below the peaks and ridges in a landscape, divided by the surface area. Small and Anderson

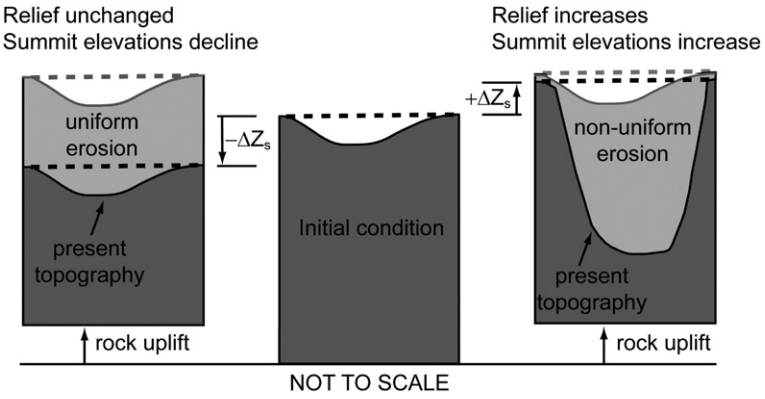

Fig. 1. Two cases of valley erosion with contrasting relief development. Centre panel represents initial condition. Geophysical relief is the mean elevation difference between a smooth surface connecting the highest points in the landscape (dashed line) and the topography. When erosion (pale shaded area) is spatially uniform (left panel), there is no change in geophysical relief, and the sum of erosionally driven rock uplift and summit erosion results in lower summit elevations ($-\Delta Z_s$). When erosion is spatially variable (right panel), there is a notable increase in geophysical relief, and changes in summit elevation are positive ($+\Delta Z_s$) because rock uplift is greater than summit erosion. Rock uplift is the same in each case because average erosion, which drives rock uplift, is equal (shaded areas are the same size) (after Small and Anderson, 1998).

(1998) demonstrated that, if remnants of a pre-erosion surface are preserved, one can estimate both geophysical relief and the total amount and distribution of erosion. Brocklehurst and Whipple (2002) described a similar approach to measuring the modern geophysical relief structure. Their "sub-ridgeline relief" indicates the difference in elevation between the valley floor and a ridgeline-related reference surface at every point in the basin. Thus it is an objective, quantitative measure of the spatial distribution of relief, although it does not necessarily indicate the amount of material eroded from the landscape. The pursuit of a more detailed understanding of how relief in glaciated landscapes relates to the extent of ice occupation and ice thickness resulted in the identification and measurement of a number of different components of relief, as illustrated in Fig. 2. While scarce in fluvial landscapes (e.g., Wobus et al., 2006; Crosby and Whipple, in revision), hanging valleys are a component of relief characteristic of glaciated landscapes (e.g., MacGregor et al., 2000; Amundson and Iverson, 2006), and hold the potential to add a considerable amount of relief to the landscape.

Whipple et al. (1999) proposed the following mechanisms whereby glacial erosion might increase the relief in a previously fluvially-sculpted landscape (see Whipple et al., 1999, Fig. 5): valley widening, ice buttressing of rock slopes, and formation of hanging valleys and overdeepenings. Furthermore, Whipple et al. (1999) suggested that the potential relief increase due to ice buttressing, the width of parabolic glacial valley cross-sections and the relief production due to hanging valleys should all depend on ice thickness. Implicit in the argument for relief production associated with hanging valleys to scale with ice thickness is the assumption that there are not major icefalls at tributary junctions during a glacial maximum. Whipple et al. (1999) argued that relief grows because ponding of ice from the tributaries against the thicker ice of the main glacier limits erosion on the tributaries. This contrasts with the process envisioned by MacGregor et al. (2000), and Amundson and Iverson (2006), who argue that differences in ice flux cause differences in trunk and tributary erosion rates which drive the formation of hanging valleys, and ultimately set their height. Following this approach, hanging valley height grows with time, limited only by the duration of ice occupation. The common observation that the trimlines of tributary ice streams grade smoothly into trunk valley ice stream trimlines, however, suggests that there is a limit to the growth of glacial hanging valley relief that may well relate to trunk glacier ice thickness as suggested by Whipple et al. (1999). The nature of this limit to hanging valley growth is not yet fully understood: ice and erosion dynamics associated with hanging valleys are complex, and many questions remain (e.g., Jason Amundson and Neal Iverson, pers. comm.). Fully 3D dynamic models of the interaction of tributary and mainstem glaciers seem a fruitful avenue to pursue in this regard. We seek an understanding of how glaciation affects relief development rather than a detailed understanding of hanging valley formation, which is beyond the scope of this study.

Acting in direct opposition to these relief-production mechanisms, Whipple et al. (1999) envisioned three

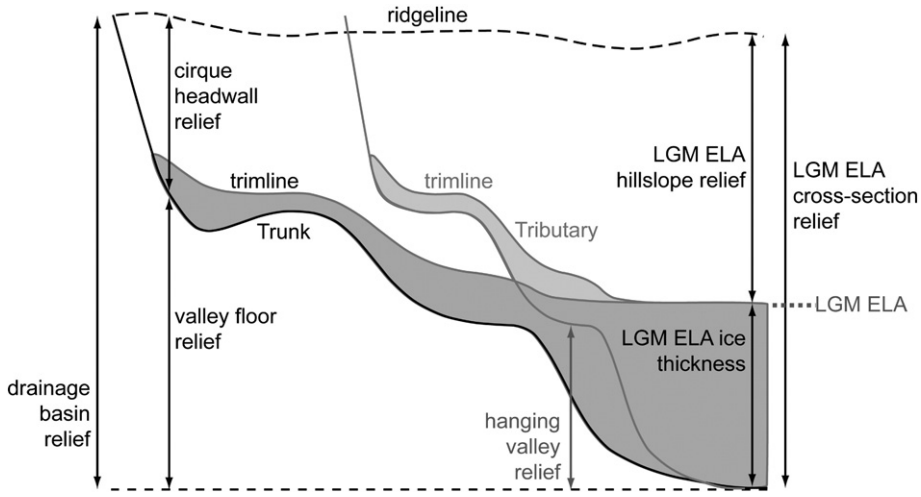

Fig. 2. Schematic illustration of definitions of relief used here. All except hanging valley relief are for the trunk valley; hanging valley relief is measured for tributaries. At the ELA, ice surface contours are assumed to be straight across the valley, so the height of the trimline above the thalweg gives the centreline ice thickness.

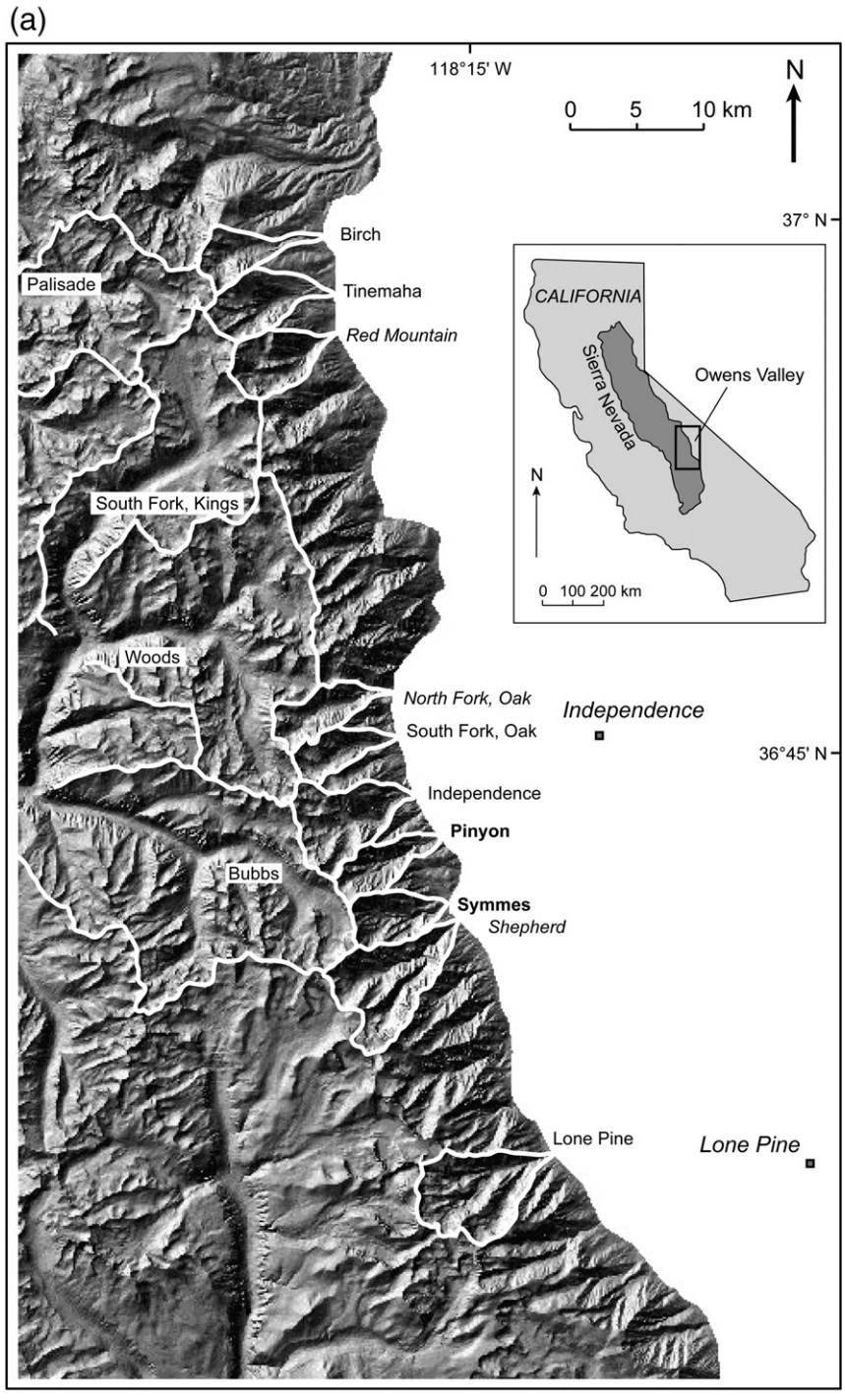

Fig. 3. (a) Shaded relief map of the study site in the Sierra Nevada, California, highlighted on the inset map. Drainage basins studied outlined in white. On the eastern side of the range, three categories of basin, based on the degree of glaciation at the Last Glacial Maximum, are illustrated as follows: nonglaciated (bold), moderate glaciation (italic) and full glaciation (regular). Select basins on the western side of the range, as listed in Table 2, are also highlighted. (b) Shaded relief map of the study site in the Sangre de Cristo Range, Colorado, highlighted on the inset map. Key as in Fig. 3a. Simplified structure after Johnson et al. (1987). Map shows the major folds and faults in the region of interest; subsidiary faults and folds have the same general orientation. CLA — Cotton Lake Anticline; GPS — Gibson Peak Syncline; MMT — Marble Mountain Thrust.

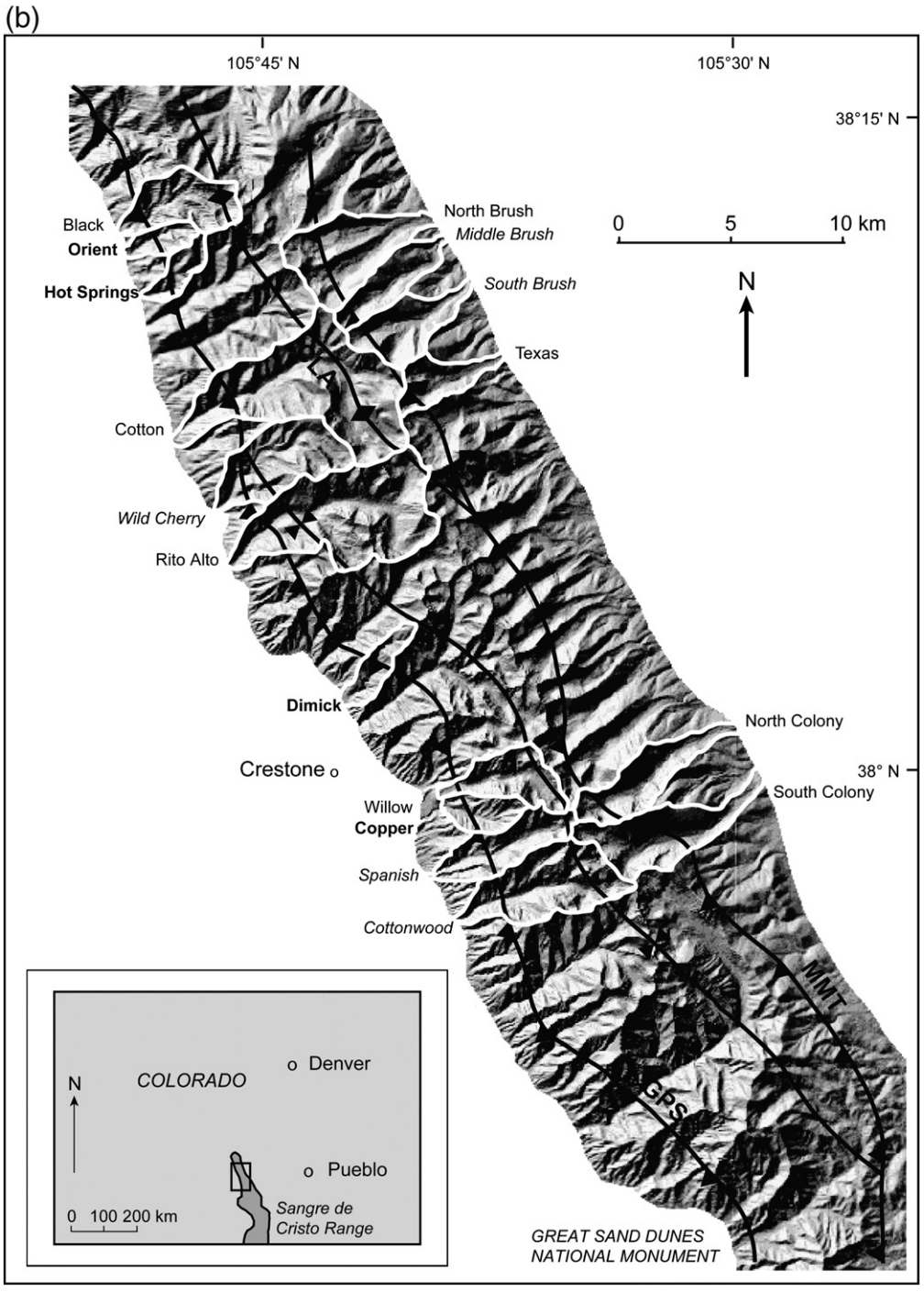

Fig. 3 (*continued*).

relief reduction mechanisms: concentration of erosion at higher elevations, reduction of fluvial erosion downstream of glaciers, and acceleration of summit-lowering rates in the periglacial regime. Brocklehurst and Whipple (2002) determined that the glaciers of the eastern Sierra Nevada have been responsible for relief production only where glaciers have been able to enlarge drainage basins through headwall erosion into relatively low-relief topography. However, in all cases glaciers were responsible for redistribution of relief compared with their

fluvially-sculpted, nonglaciated counterparts, and thus at least some of both the relief production and relief reduction mechanisms must be active.

3. Field sites

We carried out fieldwork and determined relief estimates in two ranges in the western US, the Sierra Nevada in California, and the Sangre de Cristo Range in southern Colorado. The section of the Sierra Nevada of interest (Fig. 3a) encompasses the eastern side of the range (ten drainage basins) and the headwaters of four of the basins draining to the west. This region comprises homogeneous Cretaceous granodiorites and quartz monzonites (Moore, 1963; Bateman, 1965; Moore, 1981). Present-day tectonic activity is dominated by strike-slip motion on the Owens Valley Fault farther to the east. However, the eastern range-front normal fault may still be active, contributing to fairly uniform uplift rates on the order of ~0.2 mm/yr (Gillespie, 1982). The glacial history of the range has been the focus of numerous studies (e.g., Mathes, 1930; Wahrhaftig and Birman, 1965; Gillespie, 1982; Burbank, 1991; Clark et al., 1994; Clark and Gillespie, 1997; Benson et al., 1998). The eastern side of the Sierra Nevada (Brocklehurst and Whipple, 2002) is more directly comparable with the Sangre de Cristo Range in terms of drainage basin scale, while considering the western side of the Sierra Nevada allowed us to extend the range of ice thicknesses studied.

The section of the Sangre de Cristo Range of interest is illustrated in Fig. 3b, comprising eleven drainage basins on the western side, and six to the east. The rocks here comprise Palaeozoic sedimentary units and Precambrian metamorphic rocks (Johnson et al., 1987). The tectonic regime in the Sangre de Cristo Range is also consistent throughout the region of interest. The normal component of slip rates at the range front has averaged around 0.1–0.2 mm/yr during the late Pleistocene (McCalpin, 1986, 1987), comparable to rates measured in the Sierra Nevada. Inactive folds and thrust faults dominate the internal structure of the range, with a trend subparallel to the strike of the range (Fig. 3b) (Johnson et al., 1987). Spectacular moraines on the eastern side of the range (e.g., Johnson et al., 1987) imply substantially more glacial erosion on this side of the range, presumably reflecting the effects of wind-blown snow crossing the range from west to east (e.g., Brocklehurst and MacGregor, 2005), and the North American monsoon system bringing precipitation from the Gulf of Mexico (e.g., Higgins et al., 1997; Poore et al., 2005). The glacial history is summarised by McCalpin (1981), while additional research has focussed on cirque evolution (e.g., Olyphant, 1981) and rock glaciers (e.g., Burger et al., 1999).

We divided the drainage basins into three categories on the basis of the degree of glaciation experienced at the LGM (see below). This represents a proxy for relative ice extent throughout the Quaternary, but not the average conditions during the Quaternary (Porter, 1989), which are most obviously reflected in the modern landscape (Brocklehurst and Whipple, 2002). "Full glaciation" symbolizes LGM glaciers extending to the range front, "partial glaciation" indicates significant LGM glaciers which did not reach the range front, and "fluvial/nonglacial" indicates no significant occupation by ice during the Quaternary.

We conducted a further exploration of sub-ridgeline relief in two more apparently asymmetric ranges, the Bitterroot Range in Idaho/Montana (e.g., Ruppel et al., 1993), and the Teton Range in Wyoming (e.g., Roberts and Burbank, 1993; Byrd et al., 1994). Both again exhibit much more substantial moraines on the eastern side of the range, but whereas the section of the Bitterroot Range of interest has been largely tectonically inactive during the Quaternary, the range-bounding normal fault on the east side of the Teton Range has been moving rapidly, at rates up to 2.2 mm/yr (Pierce, 1999).

4. Methods

As outlined above, our twin aims were to compare various metrics of relief with LGM ELA ice thickness (as a proxy for mean Quaternary ice thicknesses) to test the hypothesis that relief production scales with ice thickness in glaciated landscapes (Whipple et al., 1999), and to examine in detail the variations in relief structure as a function of degree of glaciation. Our methods combine aerial photograph interpretation and field mapping with measurements taken from USGS 1:24,000 topographic maps and USGS 30 m digital elevation model (DEM) data.

The relationships between the measures of relief employed here (Fig. 2) and the relief production and reduction mechanisms of Whipple et al. (1999) are summarised in Table 1. In terms of relief production, all else being equal, if a valley widens from a V-shaped cross-section to a U-shape, there will be an accompanying increase in sub-ridgeline, or geophysical, relief, i.e., the 'missing mass' within the drainage basin will increase. Widening of the valley at the expense of low relief topography may increase hillslope relief. If ice buttressing allows taller hillslopes, this will result in an increase in both sub-ridgeline relief and valley cross-

Table 1
Relief production/reduction mechanisms and related measures of relief

Relief change	Relevant relief measures
Relief production	
Valley widening	Sub-ridgeline, LGM ELA hillslope
Ice buttressing	Sub-ridgeline, LGM ELA hillslope
Hanging valleys	Sub-ridgeline, hanging valley, valley floor, drainage basin
Relief reduction	
High elevation valley floor erosion	Valley floor, drainage basin
Reduced fluvial erosion downstream	Not tested here
Summit lowering	Cirque headwall, LGM ELA hillslope, sub-ridgeline, drainage basin

section relief. Introducing hanging valleys and glacial steps evidently introduces hanging valley relief into the landscape, and can potentially cause increases in geophysical relief and drainage basin relief.

Erosion focused in the valley floor above the LGM ELA (e.g., Brocklehurst and Whipple, 2002) will act to reduce valley floor relief, and (assuming there is no change in headwall relief) drainage basin relief. Enhanced bedrock weathering rates by periglacial processes will act to reduce cirque headwall, LGM ELA hillslope, and sub-ridgeline relief. None of our measures here addresses the potential for increased sedimentation downstream of a glaciated valley reducing drainage basin relief.

4.1. Field methods

The trimline marks the boundary on the valley wall between rock that was beneath ice during a glaciation, and rock that was exposed subaerially above the trimline (e.g., periglacial trimline of Benn and Evans, 1998). Thus the trimline is an indicator of ice thickness. Typically, the trimline separates smooth, glacially-polished rock below from more jagged outcrops above. We focussed on the most prominent trimline, the one from the LGM, to determine a proxy for ice thickness to compare with our relief estimates. It is well established in the Sierra Nevada that the 'Tioga' (LGM) is one of the most extensive glaciations in the history of the range, with a very similar extent to the 'Tenaya' glaciation that preceded it, while recent glaciations (e.g., Recess Peak) have been much less widespread (Wahrhaftig and Birman, 1965; Clark and Gillespie, 1997). Therefore it seems reasonable to assume that the prominent trimlines mapped represent the LGM. Glacial studies in the Sangre de Cristo Range have been less comprehensive, but the same assumption appears appropriate. In some cases, trimlines from these more recent glaciations were also present, at lower positions on the valley wall, in the upper reaches of the valley, but trimline remnants from earlier glaciations lying above the LGM trimlines were rare. Our trimline mapping was conducted initially on the basis of aerial photograph and topographic map interpretation, verified with field observations. In practice, there were two principle means of identifying the trimline. Firstly, the trimline often represented a break in slope between steeper valley sides below and shallower slopes above, although this was not always the case; sometimes the LGM trimline lay within a steep cliff. Secondly, the trimline was often close to the top of, or inferred to be partially buried by, talus cones forming against the valley wall (Gillespie, 1982). Fig. 4 shows examples of trimlines from the eastern Sierra Nevada and the western Sangre de Cristo Range. Below the LGM ELA, we determined the margins of the glacier from lateral and terminal moraines, using field observations to supplement previously published mapping (e.g., Gillespie, 1982; Johnson et al., 1987) and aerial photograph interpretation, again attempting to focus on features related to the LGM glaciation. Fig. 5 illustrates the LGM glacier outline determined for Independence Creek in the Sierra Nevada (see Fig. 3a).

4.2. LGM ELA ice thickness

We used the accumulation-ablation area ratio method with a ratio of 0.65 (e.g., Meierding, 1982) to estimate ELAs from our mapped glacier outlines. Each of these gives a local estimate of the ELA; our estimates were consistent among partially and fully glaciated drainage basins along a particular side of a mountain range, and also consistent with published measurements (McCalpin, 1981; Gillespie, 1982; Burbank, 1991). For our comparison with relief measurements in nonglaciated drainage basins, we assumed that the consistent estimates reflect a regional ELA, and used this, rather than the local ELA, which would obviously have been much higher (how this reference level is used in nonglaciated basins is explained below). The exception to this approach was in the western Sierra Nevada, where we did not map the entirety of the larger glaciers, rather we use an LGM ELA of 2800 m above sea level (m asl) (Burbank, 1991). We used the assumption that ice surface contours at the LGM ELA would have trended in a straight line across the valley (e.g., Benn and Evans, 1998) to then estimate the centreline ice thickness, the difference in elevation between the LGM ELA ice surface contour and the current thalweg. This implicitly assumes negligible removal of sediment,

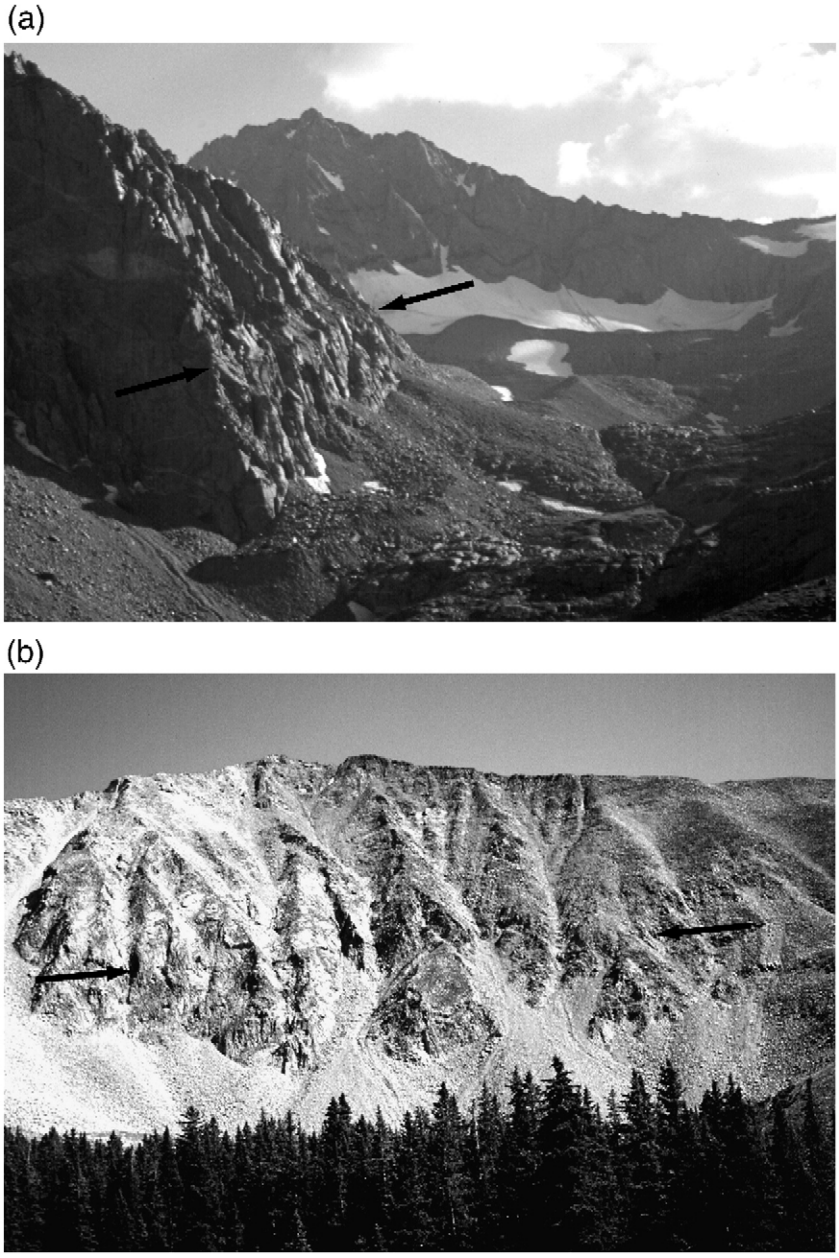

Fig. 4. Photographs of typical trimlines in the field. (a) Birch Creek, eastern Sierra Nevada. Prominent trimline, indicated by arrows, occurs at the break in slope at the top of the vertical cliff-face. (b) Black Canyon, Sangre de Cristo Range. Trimline is typically more difficult to identify in the Sangre de Cristo Range. In this case the trimline, indicated by arrows, lies just above the top of the tallest talus cones.

bedrock incision, or deposition on the valley floor since the last glaciation, which at the resolution of our measurements is a reasonable approximation.

4.3. Topographic analyses

With the exception of sub-ridgeline relief, our classification scheme for relief ('point' measurements) is given in Fig. 2, and we determined these different measures of relief from 1:24,000 scale topographic maps. Given that our measurements are taken from topographic maps, the resolution is no greater than half the contour interval (i.e., 10 m (California) or 20 ft (Colorado)), but since this is substantially less than any of our relief measurements, we feel this is sufficient resolution for this study. Our focus is on topographic

Fig. 5. Shaded relief map of the reconstructed LGM glacier for Independence Creek, eastern Sierra Nevada (see Fig. 3a for location). Drainage basin outline in white, solid, LGM glacier outline white, dashed.

relief above the LGM ELA, since in these ranges glaciers have done little to modify the landscape below this elevation (Brocklehurst and Whipple, 2002, 2006). LGM ELA hillslope relief is the difference in elevation between the trimline at the LGM ELA and the higher of the two ridgelines for the valley cross-section drawn perpendicular to the general trend of the valley axis at the ELA. For nonglaciated basins, our comparable

Fig. 6. Photograph illustrating lithologic control on glacial landforms in the Sangre de Cristo Range. Photograph is taken looking to the south towards San Isabel Lake and the cirque at the top of the San Isabel valley. To the east (left) of the lake, the shallow hillside is parallel to the dip-slope on the sedimentary units, while to the west (right) of the lake, the hillside that cuts across the bedding in the sedimentary units is noticeably steeper.

Table 2
Summary of point measures of relief from topographic maps

Basin	Degree of glaciation at LGM	Drainage area [km^2]	LGM ELA estimate [m asl]	LGM ELA ice thickness [m]	LGM ELA hillslope relief [m]	LGM ELA cross section relief [m]	Hanging valley relief [m]	Valley floor relief [m]	Headwall relief [m]	Drainage basin relief [m]	Mean sub-ridgeline relief [m]
Eastern Sierra Nevada											
Birch	Partial	13.4	2860	110	560	670		970	510	1480	231
Independence	Full	30.4	2920	170	660	830	140	760	590	1350	233
Lone Pine	Full	31.6	2940	140	460	600	110, 140, 170	1140	400	1540	355
North Fork, Oak	Partial	20.9	2880	130	540	670	130	930	300	1230	223
South Fork, Oak	Full	10.0	2860	130	520	650		840	350	1190	186
Pinyon	None	12.6	–	0	700	700		760	360	1120	252
Red Mountain	Full	16.9	2800	80	640	720		920	520	1440	299
Shepherd	Partial	36.0	3000	120	1040	1160	110, 110	1030	330	1360	270
Symmes	None	11.8	–	0	700	700		800	440	1240	262
Tinemaha	Full	14.9	2840	90	640	730	100	1030	300	1330	260
Western Sierra Nevada											
Bubbs	Full	*	2800**	240	820	1060	270, 280, 320, 320, 360	1300	360	1660	*
South Fork, Kings	Full	*	2800**	220	1120	1340	250, 260, 270, 280, 300, 330	1220	460	1680	*
Palisade	Full	*	2800**	200	920	1120	210, 250, 250, 250, 270, 280	1260	380	1640	*
Woods	Full	*	2800**	210	1060	1270	160, 170, 180, 180, 230	940	360	1300	*
Western Sangre de Cristo range											
Black	Full	10.5	3200	60	360	420	100	410	490	900	178
Copper	None	5.1	–	0	420	420		480	560	1040	133
Cotton	Full	35.3	3150	110	610	720	120, 140, 180	560	360	920	312
Cottonwood	Partial	17.3	3175	130	610	740	100, 160, 180, 200	730	220	950	233
Dimick	None	4.1	–	0	270	270		420	240	660	87
Hot Springs	None	3.2	–	0	240	240		300	230	530	97
Orient	None	3.7	–	0	440	440		240	290	530	85
Rito Alto	Full	31.3	3200	110	700	810	120, 160, 170	620	380	1000	282
Spanish	Partial	8.8	3250	60	360	420		540	570	1110	174
Wild Cherry	Partial	14.7	3320	60	450	510	120, 160	470	290	760	177
Willow	Full	9.3	3175	80	600	680		650	340	990	255
Eastern Sangre de Cristo range											
Middle Brush	Partial	9.6	3150	50	300	350		600	350	950	103
North Brush	Full	16.5	3055	100	240	340	110, 120	560	370	930	182
South Brush	Partial	10.7	3080	80	270	350		660	250	910	207
North Colony	Full	13.0	3175	120	360	480	120	780	240	1020	195
South Colony	Full	15.7	3150	180	300	480	300	840	450	1290	262
Texas	Full	7.0	3175	70	300	370		760	180	940	133

* Entire drainage basin not studied.
** From Burbank (1991).

measurement of hillslope relief has the same upper elevation, while the lower elevation is the mean thalweg elevation at the regional LGM ELA (see above). Hanging valley relief was measured between the thalweg elevation along the projected centreline of the hanging valley, and the elevation of the prominent break in slope between the shallow valley floor of the tributary and the steep step down to the trunk valley. Valley floor relief (for the trunk stream) is the difference in elevation between the thalweg at the LGM ELA (i.e., the LGM ELA minus the LGM ELA ice thickness), and the base of the cirque headwall, the prominent break in slope between the steep, uniform slope of the headwall and the shallower gradients of the cirque floor. The trimline around the cirque usually lies on the cirque headwall by this morphologic definition. For consistency, whenever a valley exhibited multiple cirques, we always chose the cirque giving maximum valley relief. In practice, the difference in valley relief measurements between cirques did not exceed 200 m. The cirque headwall relief is the difference in elevation between the base of the headwall as defined above and the highest point on the divide surrounding the cirque in question. We did not encounter any cirques with a significant slope to the base of the headwall that might otherwise cause ambiguity in these definitions. For nonglaciated catchments, we used the break between the uniform gradient of the hillslope and the downstream decreasing gradient of the fluvial/debris flow channel (e.g., Snyder et al., 2000) as the equivalent position to measure valley floor and headwall relief. Drainage basin relief is valley floor relief plus headwall relief.

Our digital topographic analyses follow methods outlined by Brocklehurst and Whipple (2002). We used a flow routing routine in ArcInfo to extract drainage network structures and individual drainage basins, in each case taking the downstream extent of the basin to lie at the range front. To analyse the distribution of relief, we followed the sub-ridgeline relief distribution method of Brocklehurst and Whipple (2002). In summary, a cubic spline surface is interpolated between the ridgelines surrounding a drainage basin (equivalent to stretching a rubber sheet across the top of the basin). This surface yields a ridgeline-related elevation at every point within the drainage basin. Any peaks within the basin that penetrate this surface are combined with the ridgelines surrounding the basin before interpolating an updated ridgeline-related surface. Subtracting the DEM from this surface yields a measure of the distance below the ridgelines for each point in the basin. Summing this 'sub-ridgeline relief' is then a measure of the 'missing mass' within the drainage basin (although not necessarily the eroded mass), and dividing this number by the drainage area yields a length-scale relief measurement comparable to 'geophysical relief' (Small and Anderson, 1998).

5. Results

5.1. Field observations

Our field observations and topographic map interpretations suggest that lithology and structural grain play a more important role in the drainage planform in the Sangre de Cristo Range than in the Sierra Nevada. Whereas drainage basins in the eastern Sierra Nevada run essentially perpendicular to the range crest/front, many of the larger drainage basins in the western Sangre de Cristo Range run parallel with the range crest in their upper reaches (Fig. 3b), which is also parallel to the main structural grain. Furthermore, the valley cross-section in the upper part of the basin in these cases is often noticeably asymmetric (Fig. 6), with a shallower hillslope gradient on one side of the valley following bedding planes within the Palaeozoic sedimentary sequence. The opposite hillslope, cut across the beds, is much steeper. Our LGM ELA estimates are given in Table 2. To summarise the regional averages: eastern side of the Sierra Nevada: 2890 m asl, western side of the Sierra Nevada: 2800 m asl (Burbank, 1991), eastern side of the Sangre de Cristo Range: 3130 m asl, and western side of the Sangre de Cristo Range: 3210 m asl.

5.2. Relief and ice thickness comparison

We note that our LGM ELA ice thickness estimates show some correlation with drainage basin area (Fig. 7).

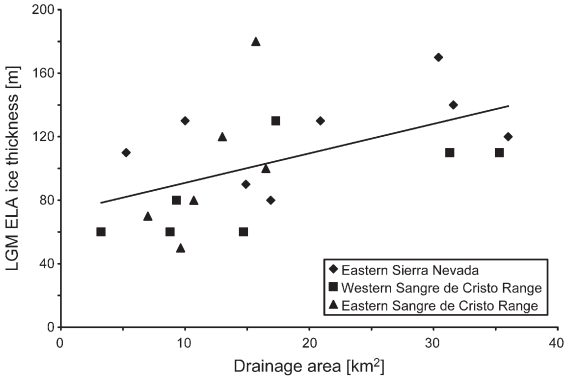

Fig. 7. LGM ELA ice thickness against drainage area for partially and fully glaciated drainage basins from the eastern side of the Sierra Nevada and the Sangre de Cristo Range. For the dataset as a whole, a linear least-squares regression has a r^2 value of 0.27.

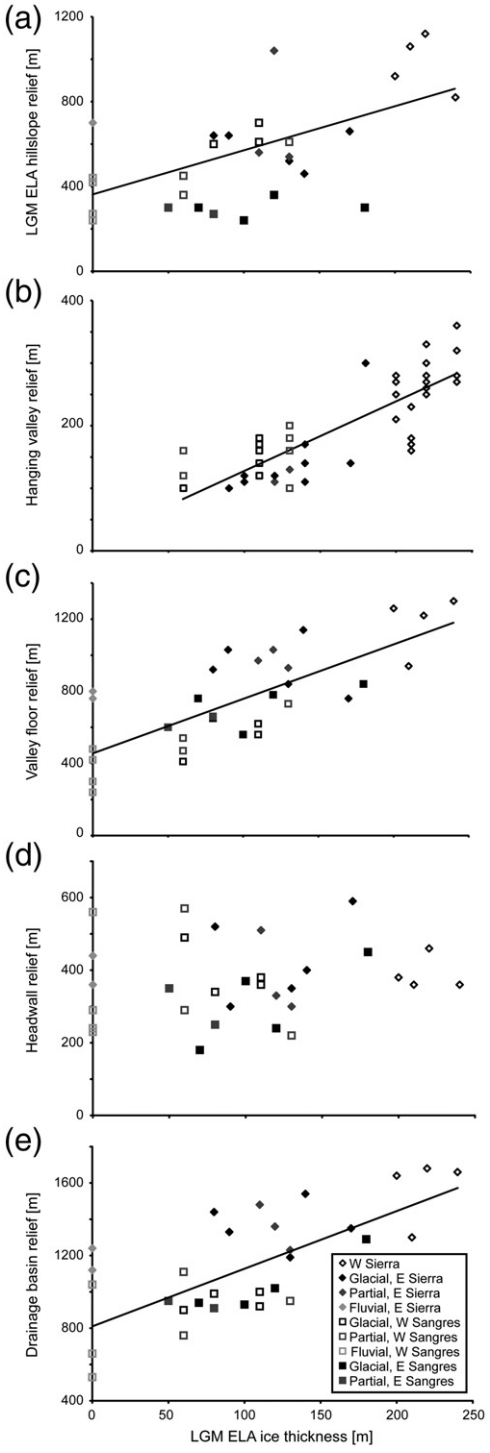

This is not a surprise; we would expect larger drainage basins to have shallower downvalley gradients and thus the potential to host thicker glaciers. This is because thickness and slope are inversely correlated because basal shear stress is consistently ~1 bar (10^5 Pa) beneath temperate glaciers (e.g., Paterson, 1994).

Fig. 8 and Table 2 summarise the results of our ice thickness calculations and various relief estimates for basins on both sides of the Sierra Nevada and the western side of the Sangre de Cristo Range. There is some scatter to the data, but trends do emerge. Hillslope relief at the LGM ELA (Fig. 8a) tends to increase as LGM ELA ice thickness increases, although a reasonable linear regression to this effect only emerges when both sides of both ranges are considered as one data set. This linear regression has an intercept within the range of hillslope relief values for nonglaciated basins in the western Sangre de Cristo Range. The two sides of the Sangre de Cristo Range are not substantially different in terms of hillslope relief at the LGM ELA, while the larger, shallower drainage basins of the western Sierra Nevada exhibit greater hillslope relief than their smaller, steeper counterparts on the eastern side of the range. LGM ELA cross-section relief has a stronger trend with ice thickness since ice thickness is part of this relief measure.

The linear trend of hanging valley relief versus LGM ELA ice thickness (Fig. 8b) again emerges most strongly when all of the data are considered together. The best fit least-squares linear regression has an intercept of 15 m, but the r^2 value only falls by 0.004 if the fit is forced through 0, which is the expectation of a fluvial landscape (neglecting the modest change in elevation associated with the valley floor gradient between the measurement points in a fluvial landscape equivalent to the locations used for hanging valley height calculations). Again, greater ice thicknesses on the western side of the Sierra Nevada allow more substantial hanging valley relief, but also a greater range in hanging valley heights. Due to the drainage network structure, there are very few hanging valleys on the eastern side of the Sangre de Cristo Range.

Fig. 8. Comparison of various measures of relief with LGM ELA ice thicknesses in the Sierra Nevada and the Sangre de Cristo Range. See Fig. 2 for definitions of relief measures. Where portrayed, linear least-squares regression lines are through all of the data points from both ranges. Keys for all of the panels are in (e). (a) LGM ELA hillslope relief. The regression line has a slope of 2.01, an intercept of 360 m, and a r^2 value of 0.32. (b) Hanging valley relief. The regression line has a slope of 1.11, an intercept of 15 m, and a r^2 value of 0.682. If the intercept is forced to be 0, the r^2 value becomes 0.678. (c) Valley floor relief. Regression line has a slope of 3.02 and a r^2 value of 0.57. (d) Headwall relief. (e) Drainage basin relief. Regression line has a slope of 3.24, and a r^2 value of 0.52.

Valley floor relief (Fig. 8c) also tends to increase as LGM ELA ice thickness increases. The most scatter occurs among nonglaciated basins, and the large basins of the western Sierra Nevada have the greatest valley floor relief. This partly reflects the lower thalweg at the LGM ELA rather than higher divides. The Sierra Nevada as a whole has greater relief than the Sangre de Cristo Range (Brocklehurst and Whipple, 2006), and this is reflected in the ~400 m greater valley floor relief above the LGM ELA in the basins of the eastern Sierra Nevada than in the Sangre de Cristo Range. Valley floor relief and drainage basin relief (of which valley floor relief is a key constituent) are the only relief measures to clearly reflect this distinction.

Headwall relief (Fig. 8d) shows no correlation with LGM ELA ice thickness, with the same range of headwall relief values across the full spectrum of LGM ELA ice thicknesses, including the nonglaciated drainage basins. Accordingly, the trends in drainage basin relief (Fig. 8e) reflect differences in valley floor relief rather than on the hillslopes, which are comparable between the Sangre de Cristo Range and the Sierra Nevada. This matches our expectation for fluvial landscapes when comparing relief to basin size.

5.3. Relief, degree of glaciation, and drainage basin size

Fig. 9 shows the relationship between mean sub-ridgeline relief and drainage area for the eastern side of the Sierra Nevada, and the Sangre de Cristo, Bitterroot and Teton Ranges. For the Sierra Nevada and Sangre de Cristo Range, the major trend is for mean sub-ridgeline relief to increase with drainage area, along nearly identical trends, for landscapes across the full spectrum of degrees of glacial modification. Furthermore, the Sangre de Cristo Range is largely symmetrical across the range in terms of mean sub-ridgeline relief, even though the pronounced moraines on the east side suggest strong asymmetry in terms of volumes of glacial erosion. In both ranges, glaciated basins have more mean relief, but this is due principally to their being larger; fluvial basins of the same size would apparently have very similar missing mass. The Bitterroot Range also has substantial moraines only along its eastern side, suggesting notable asymmetry in terms of volumes of material eroded by glaciers. While the results are somewhat more scattered, there is no evidence of any systematic difference in mean sub-ridgeline relief between the two sides of the range, and again there is no obvious distinction in missing mass between drainage basins with different degrees of glacial modification. In the Teton Range, conversely, there is a clear tendency for drainage basins on the eastern, tectonically active side of the range to have greater mean sub-ridgeline relief, but again no noticeable deviation from the same trend of mean sub-ridgeline relief versus drainage area regardless of degree of glacial modification. Fig. 9a–d are all plotted on the

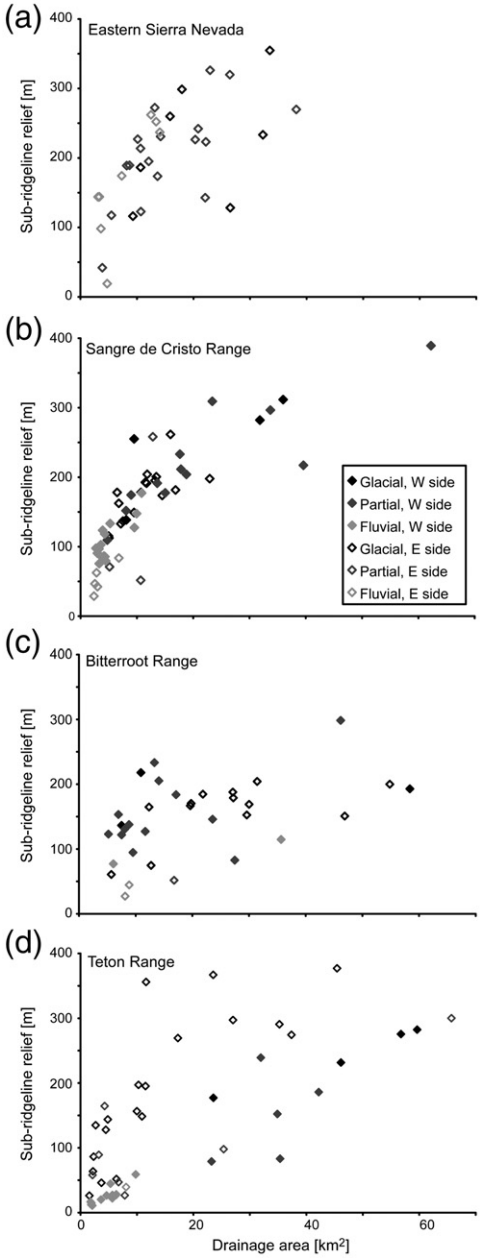

Fig. 9. Mean sub-ridgeline relief versus drainage area for non-, partially-, and fully glaciated basins, and on the east side (open symbols) or the west side (solid symbols) of a range. (a) Eastern side of the Sierra Nevada, key as in (b). (b) Sangre de Cristo Range. (c) Bitterroot Range, key as in (b). (d) Teton Range, key as in (b).

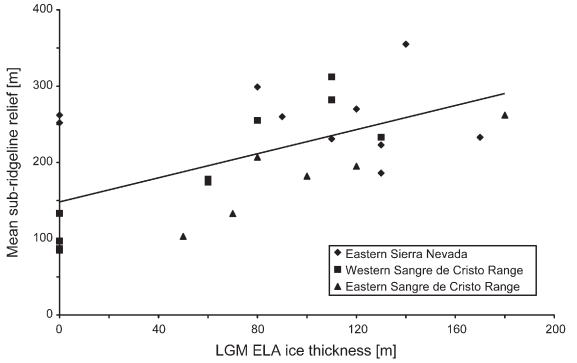

Fig. 10. Mean sub-ridgeline relief versus LGM ELA ice thickness for all drainage basins in the eastern side of the Sierra Nevada and the Sangre de Cristo Range. Linear least-squares regression through all of the data points from both ranges has a slope of 0.76 and a r^2 value of 0.33. Taken separately, linear least-squares fits for the western and eastern sides Sangre de Cristo Range have slopes of 1.48 and 1.09 and r^2 values of 0.85 and 0.80 respectively.

same axes: a few drainage basins on the east side of the Teton Range have greater mean sub-ridgeline relief for a given drainage area, and some of the basins on the west of the Teton Range, and in the Bitterroot Range, have less mean sub-ridgeline relief, but otherwise the different ranges all plot in much the same places.

Fig. 10 illustrates the relationship between mean sub-ridgeline relief and LGM ELA ice thickness, where a trend is expected because larger drainage basins will have shallower downvalley gradients and thicker ice (see above), and are also associated with greater mean sub-ridgeline relief. Interestingly, the relationship is much clearer for the drainage basins of the Sangre de Cristo Range than it is for the eastern Sierra Nevada.

6. Discussion

We have conducted both 'point' and 'volume' measures of relief to elucidate the key distinctions between landscapes exhibiting different degrees of glaciation in terms of glacier extent, and different volumes of glacial erosion. Given that the shallower downvalley gradients of larger drainage basins allow thicker glaciers to develop in wider valleys, it is perhaps not surprising that at least some of the point measurements of relief appear to correlate with ice thickness. Meanwhile the volume measure of relief (mean sub-ridgeline relief) correlates with both drainage area and ice thickness. The former is anticipated because larger drainage basins will tend to be wider and deeper, while the latter is a corollary of the relationship between downvalley slope (a reflection of drainage basin area) and ice thickness. However, the story is not necessarily straightforward.

We have found that hillslope and cross-section relief at the ELA, hanging valley relief, and valley floor relief scale with LGM ELA ice thickness. The valley floor relief partly reflects lower LGM ELA valley thalwegs beneath thicker ice. Also, the divides at the top of the drainage basins on the western side of the Sierra Nevada must be at the same heights as those reached by the drainage basins on the eastern side of the range, so part of the difference in drainage basin relief must be an artefact of the specific cirques chosen, that is with more cirques to choose from, those selected from the western side of the range were higher than their eastern counterparts. Furthermore, the valley floor relief is less than that which would be expected under continuous fluvial conditions during the Quaternary (Brocklehurst and Whipple, 2002, 2006). Hillslope relief at the ELA again may reflect basic geometry; larger drainage basins with thicker ice will tend to have greater separation between the ridgelines on opposite sides of the basin, allowing greater hillslope relief. Also, in shorter, steeper basins, the ELA lies closer to the range front than in longer, shallower basins, placing a limit on potential hillslope relief. LGM ELA cross-section relief, combining LGM ELA ice thickness with hillslope relief, will also therefore scale with ice thickness. Our evidence supports the close association between ice thickness and hanging valley relief, proposed by Whipple et al. (1999). Whipple et al. (1999) suggested that this was a result of ponding of tributary ice against the trunk glacier. However, we cannot at this stage discount the suggestion that tributary relief is controlled by differences in ice flux (MacGregor et al., 2000; Amundson and Iverson, 2006). There is an obvious need for further research to determine what apparently limits hanging valley relief. While larger, thicker, trunk glaciers are likely to have a greater contrast in ice flux with their small tributaries, hanging valleys do not seem to grow without limits. It is possible that we are only looking at a snapshot of evolving glacial landscapes, or that some other factor relating to ice dynamics acts to limit relief production.

Our analyses indicate that the glaciated landscapes of the eastern Sierra Nevada and Sangre de Cristo Range look broadly very similar. The principal distinctions between the two are the reduced drainage basin relief in the Sangre de Cristo Range, and the greater degree of lithologic and structural control on landscape evolution in the Sangre de Cristo Range. Here, the upper reaches of the larger basins are range-parallel, following the structural grain. It is difficult to evaluate when the drainage network took on this planform, which could well have occurred prior to the onset of glaciation in the range. However, the lithology clearly plays a key role in the evolution of the glaciated landscape. The cross-sections of these valley

heads are asymmetric, as the valley walls on one side lie at a shallower angle parallel to bedding planes, while the valley walls opposite are noticeably steeper with angular steps cutting across each of the bedding planes. Despite the clear lithologic variations, however, in terms of volume of missing mass, the Sierra Nevada and the Sangre de Cristo Range are indistinguishable.

Mean sub-ridgeline relief is a function of drainage area, because larger drainage basins tend to be wider and deeper. The transition from fluvial to glacial landscape does not in itself lead to a noticeable change in mean sub-ridgeline relief. Given the clear differences between the two landscapes, this is perhaps surprising, but it indicates that both relief production and relief reduction mechanisms (Whipple et al., 1999) are associated with the onset of glaciation. For example, while hanging valleys develop, generating relief, valley floor relief above the hanging valley step is reduced by enhanced high level erosion. Although drainage basin relief in the eastern Sierra Nevada is greater than in the Sangre de Cristo Range, mean sub-ridgeline relief in the two ranges is quite comparable. Mean sub-ridgeline relief is also very similar on the opposite sides of Sangre de Cristo Range, despite obvious differences in volume of erosion, another striking result. In both ranges, fluvial drainage basins lie on the same trend as glaciated basins, so that glaciers are responsible for net relief production only in their ability to enlarge formerly fluvial basins at the expense of low relief topography (Brocklehurst and Whipple, 2002, 2006). The Bitterroot Range again exhibits striking asymmetry of glacial erosion but symmetry of mean sub-ridgeline relief. This appears to imply that, at least in these ranges, broadly speaking the whole of the landscape is being lowered at comparable rates, rather than erosion being focussed solely in valley floors. It is only in the Teton Range, rapidly tilting due to normal faulting, that there is across-range asymmetry (approximate doubling) in mean sub-ridgeline relief. This relief production on the eastern side of the range may contribute to flexural uplift.

The cirque headwall results presented here suggest that in the Sierra Nevada and Sangre de Cristo Range there is a characteristic height (and length) to hillslopes in glaciated landscapes which is rarely exceeded. However, periglacial hillslopes in the Himalayas (Anderson, 2005; Brocklehurst and Whipple, in review), for example, have much greater relief, suggesting a major difference in erosion conditions and rates here, such as slowly-eroding high altitude deserts (Harper and Humphrey, 2003). Our results suggest that hanging valley relief is related to trunk glacier ice thickness, but even on the western side of the Sierra Nevada, the glaciers studied here are comparatively thin. Ranges with larger glaciers, such as the Alps and Himalayas, where valley glacier ice thicknesses approach 1 km, may show a different relationship between ice thickness and hanging valley relief. The results presented here suggest that landscapes in the Alps should have greater relief than the glaciated ranges studied in the western USA, but the partitioning of this between hillslope and hanging valley relief may not be straightforward.

7. Conclusion

The onset of glaciation triggers both relief production and relief reduction mechanisms in previously fluvial landscapes. Hanging valleys, and ice buttressing and lengthening of hillslopes generate relief, more so in larger basins with thicker ice. However, in the Sierra Nevada and Sangre de Cristo Range, cirque headwall relief (or hillslope relief at the channel head) does not appear to change as a function of ice thickness/drainage basin size. Although valley floor and drainage basin relief increase with drainage basin size, this is by less than would be expected for fluvial landscapes. Sub-ridgeline relief averages the different components of relief, and as a function of drainage area lies on the same trend for both fluvial and glacial landscapes. Therefore glaciers are only responsible for net relief production if they enlarge basins at the expense of low relief topography. Hanging valley relief is correlated with glacier thickness, although the cause of this is yet to be fully explained. Much of the increased hillslope and valley floor relief in drainage basins with thicker glacial ice reflects the larger size of these basins. Mean sub-ridgeline relief is surprisingly not related to the volume of material removed by glacial erosion, but for the Teton Range appears to be affected by the particularly active tectonics.

Acknowledgements

This work was supported by a NASA GSFC Graduate Student Research Grant, NSF grant EAR-9980465 (to KXW), a GSA Fahnestock Award, a NASA Graduate Fellowship, a CIRES Visiting Fellowship, and Nuffield Foundation Award NAL/00941/G (all to SHB). We would like to thank Ryan Ewing and Noah Snyder for assistance in the field, Ben Crosby and Darryl Granger for detailed comments on early drafts of this manuscript, and Peter van der Beek and Ola Fredin, for thorough and constructive reviews.

References

Amundson, J.M., Iverson, N.R., 2006. Testing a glacial erosion rule using hang heights of hanging valleys, Jasper National Park, Alberta, Canada. Journal of Geophysical Research 111 (F01020). doi:10.1029/2005JF000359.

Anderson, R.S., 2005. Teflon peaks: the evolution of high local relief in glaciated mountain ranges. Eos Trans. AGU 86 (52), Fall Meet. Suppl., Abstract H33F-04.

Bateman, P.C., 1965. Geology and tungsten mineralization of the Bishop District, California. U.S. Geological Survey Professional Paper vol. 470 208 pp.

Benn, D.I., Evans, D.J.A., 1998. Glaciers and Glaciation. Arnold, London. 734 pp.

Benson, L.V., May, H.M., Antweiler, R.C., Brinton, T.I., Kashgarian, M., Smoot, J.P., Lund, S.P., 1998. Continuous lake-sediment records of glaciation in the Sierra Nevada between 52,600 and 12,500 14C yr B.P. Quaternary Research 50, 113–127.

Brocklehurst, S.H., Whipple, K.X., 2002. Glacial erosion and relief production in the eastern Sierra Nevada, California. Geomorphology 42 (1–2), 1–24.

Brocklehurst, S.H., MacGregor, K.R., 2005. The role of wind in the evolution of glaciated mountain ranges: field observations and insights from numerical modelling. Eos Trans. AGU 86 (52), Fall Meet. Suppl., Abstract H51C-0390.

Brocklehurst, S.H., Whipple, K.X., 2006. Assessing the relative efficiency of fluvial and glacial erosion through fluvial landscape simulation. Geomorphology 75, 283–299.

Brocklehurst, S.H., Whipple, K.X., in review. The response of glacial landscapes to spatial variations in rock uplift rate.

Burbank, D.W., 1991. Late quaternary snowline reconstructions for the southern and central Sierra Nevada, California and a reassessment of the "Recess Peak Glaciation". Quaternary Research 36, 294–306.

Burger, K.C., Degenhardt Jr., J.J., Giardino, J.R., 1999. Engineering geomorphology of rock glaciers. Geomorphology 31 (1–4), 93–132.

Byrd, J.O.D., Smith, R.B., Geissman, J.W., 1994. The Teton fault, Wyoming: topographic signature, neotectonics, and mechanisms of deformation. Journal of Geophysical Research 99 (B10), 20095–20122.

Clark, D.H., Gillespie, A.R., 1997. Timing and significance of late-glacial and Holocene cirque glaciation in the Sierra Nevada, California. Quaternary International 38–39, 21–38.

Clark, D.H., Clark, M.M., Gillespie, A.R., 1994. Debris-covered glaciers in the Sierra Nevada, California, and their implications for snowline reconstructions. Quaternary Research 41, 139–153.

Crosby, B.T., Whipple, K.X., in revision. Formation of fluvial hanging valleys: theory and simulation. Journal of Geophysical Research.

Fredin, O., 2004. Mountain centered icefields in Northern Fennoscandia. PhD thesis, Department of Physical Geography and Quaternary Geology, Stockholm University, Thesis No. 29, Stockholm, 77 pp.

Gillespie, A.R., 1982. Quaternary glaciation and tectonism in the Southeastern Sierra Nevada, Inyo County, California. PhD thesis, California Institute of Technology, Pasadena, 695 pp.

Harper, J.T., Humphrey, N.F., 2003. High altitude Himalayan climate inferred from glacial ice flux. Geophysical Research Letters 30 (14). doi:10.1029/2003GL017329.

Higgins, R.W., Yao, Y., Wang, X.L., 1997. Influence of the North American monsoon system on the U.S. summer precipitation regime. Journal of Climate 10, 2600–2622.

Johnson, B.R., Lindsey, D.A., Bruce, R.M., Soulliere, S.J., 1987. Reconnaissance geologic map of the Sangre de Cristo Wilderness Study Area, south-central Colorado. USGS Miscellaneous Field Studies Map, MF-1635-B.

Kleman, J., Stroeven, A.P., 1997. Preglacial surface remnants and Quaternary glacial regimes in northwestern Sweden. Geomorphology 19 (1–2), 35–54.

Kleman, J., Stroeven, A.P., Lundqvist, J., 2008. Quaternary ice sheet erosion and deposition in Fennoscandia. Geomorphology 97, 73–90 (this volume).

Koons, P.O., 1995. Modeling the topographic evolution of collisional belts. Annual Review of Earth and Planetary Sciences 23, 375–408.

MacGregor, K.R., Anderson, R.S., Anderson, S.P., Waddington, E.D., 2000. Numerical simulations of glacial valley longitudinal profile evolution. Geology 28 (11), 1031–1034.

Mancktelow, N.S., Grasemann, B., 1997. Time-dependent effects of heat advection and topography on cooling histories during erosion. Tectonophysics 270, 167–195.

Mathes, F.E., 1930. Geologic history of the Yosemite Valley. USGS Professional Paper, 160.

McCalpin, J.P., 1981. Quaternary geology and neotectonics of the west flank of the northern Sangre de Cristo Mountains, south-central Colorado. PhD Thesis, Colorado School of Mines, Golden, CO, 287 pp.

McCalpin, J.P., 1986. Quaternary tectonics of the Sangre de Cristo and Villa Grove Fault Zones. Colorado Geological Survey 28, 59–64 (Special Publication).

McCalpin, J.P., 1987. Recurrent quaternary normal faulting at Major Creek, Colorado: an example of youthful tectonism on the eastern boundary of the Rio Grande Rift Zone. In: Beus, S.S. (Ed.), Geological Society of America Centennial Field Guide — Rocky Mountain Section. Geological Society of America, pp. 353–356.

Meierding, T.C., 1982. Late Pleistocene glacial equilibrium-line altitudes in the Colorado Front Range: a comparison of methods. Quaternary Research 18, 289–310.

Molnar, P., England, P., 1990. Late Cenozoic uplift of mountain ranges and global climate change: chicken or egg? Nature 346, 29–34.

Montgomery, D.R., 1994. Valley incision and the uplift of mountain peaks. Journal of Geophysical Research 99, 13913–13921.

Montgomery, D.R., 2002. Valley formation by fluvial and glacial erosion. Geology 30 (11), 1047–1040.

Moore, J.G., 1963. Geology of the Mount Pinchot quadrangle, Southern Sierra Nevada, California. US Geological Survey Bulletin 1130 152 pp.

Moore, J.G., 1981. Geologic map of the Mount Whitney Quadrangle, Inyo and Tulare Counties, California. US Geological Survey Map, GQ-1545.

Olyphant, G.A., 1981. Allometry and cirque evolution. Geological Society of America Bulletin 92, 679–685.

Paterson, W.S.B., 1994. The physics of glaciers. Pergamon, Oxford, England; Tarrytown, N.Y., 480 pp.

Pierce, K.L., 1999. Fault Number 768c, Teton Fault, Central Section, Quaternary Fault and Fold Database of the United States. USGS: http://earthquakes.usgs.gov/regional/qfaults.

Poore, R.Z., Pavich, M.J., Grissino-Mayer, H.D., 2005. Record of the North American southwest monsoon from Gulf of Mexico sediment cores. Geology 33 (3), 209–212.

Porter, S.C., 1989. Some geological implications of average quaternary glacial conditions. Quaternary Research 32, 245–261.

Raymo, M.E., Ruddiman, W.F., 1992. Tectonic forcing of late Cenozoic climate. Nature 359, 117–122.

Roberts, S.V., Burbank, D.W., 1993. Uplift and thermal history of the Teton Range (northwestern Wyoming) defined by apatite fission-track dating. Earth and Planetary Science Letters 118 (1–4), 295–309.

Ruppel, E.T., O'Neill, J.M., Lopez, D.A., 1993. Geologic map of the Dillon 1x2 (degrees) quadrangle, Idaho and Montana. USGS Miscellaneous Investigations, I-1803-H.

Schuster, D.L., Ehlers, T.A., Rusmore, M.E., Farley, K.A., 2005. Rapid glacial erosion at 1.8 Ma revealed by 4He/3He Thermochronometry. Science 310, 1668–1670.

Small, E.E., Anderson, R.S., 1998. Pleistocene relief production in Laramide mountain ranges, western United States. Geology 26, 123–126.

Snyder, N.P., Whipple, K.X., Tucker, G.E., Merritts, D.J., 2000. Landscape response to tectonic forcing: DEM analysis of stream profiles in the Mendocino triple junction region, northern California. Geological Society of America Bulletin 112 (8), 1250–1263.

Stüwe, K., White, L., Brown, R., 1994. The influence of eroding topography on steady-state isotherms: application to fission track analysis. Earth and Planetary Science Letters 124, 63–74.

Wahrhaftig, C., Birman, J.H., 1965. The quaternary of the Pacific Mountain System in California. In: Wright, H.E.J., Frey, D.G. (Eds.), The Quaternary of the United States. Princeton University Press, Princeton, N.J., pp. 299–340.

Whipple, K.X., Kirby, E., Brocklehurst, S.H., 1999. Geomorphic limits to climate-induced increases in topographic relief. Nature 401, 39–43.

Willett, S.D., 1999. Orogeny and orography: The effects of erosion on the structure of mountain belts. Journal of Geophysical Research 104 (B12), 28957–28981.

Wobus, C.W., Crosby, B.T., Whipple, K.X., 2006. Hanging valleys in fluvial systems: controls on occurrence and implications for landscape evolution. Journal of Geophysical Research 111 (F02017). doi:10.1029/2005JF000406.

Zeitler, P.K., Meltzer, A.S., Koons, P.O., Craw, D., Hallet, B., Chamberlain, C.P., Kidd, W.S.F., Park, S.K., Seeber, L., Bishop, M.P., Schroder Jr., J.F., 2001. Erosion, Himalayan geodynamics, and the geomorphology of metamorphism. GSA Today 11 (1), 4–9.